Simulating Macro-Porosity in Aluminum Lost Foam Castings

P. Scarber, Jr., H. Littleton
The University of Alabama at Birmingham, Birmingham, Alabama

ABSTRACT

Porosity in aluminum castings continues to be the leading cause of scrap in most of the foundries in the world. Research has shown methods of reducing both macro- and micro-porosity in open mold aluminum castings with varying levels of success. However, the filling behavior in Lost Foam Casting is significantly different from that in open mold casting and methods of reducing porosity do not have the same effects.

Casting simulation codes have been in use for the past three decades and have successfully predicted porosity in steel and other ferrous castings. Prediction of porosity in aluminum alloys is more difficult because of the longer freezing range and lack of accurate data. Combined with the complexity of thermal gradients present during Lost Foam Casting, simulation codes have failed to predict even relatively large pores in aluminum castings.

Solidification thermophysical data and a modified solidification subroutine were both developed to predict more accurately the macro-porosity in aluminum alloy Lost Foam Castings. The solidification simulations were completed in hours and the thermophysical data matches more closely to what is happening on a microstructural level.

Simulated cooling curves using the new data were much more accurate than that using published data for the same aluminum alloy system. The predicted porosity was within a few millimeters of the experimental findings and was more accurate than published data.

INTRODUCTION

Lost Foam Casting (LFC) of parts made of aluminum alloys has increased by more than 1000% over the past two decades and new LFC foundries are opening at a relatively high rate even amidst the current economic slow-down. LFC is an established method of cost savings because many assemblies that are made by separate processes can be made in a single LFC pour. There are several examples of part consolidation that is possible by LFC, and the total cost and weight savings continue to make LFC the first choice in modern casting methods. A complete understanding of all phases of the LFC process can result in almost no rejection of parts, but intermittent macro-porosity continues to be a problem.

Computer simulation of flow, fill, and solidification is a necessary step in the successful production of high-quality LFC parts. The movement of liquid metal fronts and the development of thermal gradients are not intuitive in LFC, so computer simulations, along with real-time x-ray and casting instrumentation, become vital in understanding the source of casting anomalies. However, computer simulations of anomalies in production LFC parts have not been accurate in several cases, which cast doubt on the validity of LFC casting simulations.

Simulation of casting porosity was one of the first tasks of simulation codes developed more than three decades ago. Today, most commercial casting software will accurately predict macro-porosity in open-cavity castings and some will predict convergent metal fronts in LFC, which are associated with macro-porosity. But prediction of macro-porosity in LFC castings has not been successful in all cases, mainly due to the relatively long fill times associated with LFC – as much as an order of magnitude longer than similar open cavity castings. The longer fill times result in very complex thermal gradients, particularly in aluminum – silicon alloys.

This paper details the research process employed by the University of Alabama at Birmingham, under the auspices of the American Foundry Society Lost Foam Casting Committee, to increase the accuracy of porosity prediction in aluminum LFC castings. A commercial simulation code was modified and an experimental casting matrix was developed in order to improve the accuracy of LFC casting simulations in predicting macro-porosity in LFC aluminum alloy castings. The aluminum alloys used in this study were C356 and A319, and the predicted porosity was validated on a production engine block.

THEORY

Prediction of porosity in metal alloy castings has been the goal of computer simulation of castings from its inception. Some of the first computer simulations were designed to predict macro-porosity in relatively large ferrous castings, mostly steel alloys, with simple geometries and thick sections. [1, 10] These simulations involved castings with relatively fast cooling rates and short feeding ranges and distances, so using simulations to find casting hot spots or solidification criteria such as local solidification time or solidus velocity are reasonably accurate. However, these solidification simulation methods do not produce accurate porosity predictions for aluminum-silicon alloys, which typically have long freezing ranges.

Early efforts to simulate solidification in aluminum alloys focused on models of permanent mold castings with very high cooling rates. [2-4] The relatively rapid solidification eliminated the effects of the long freezing range and negated thermal convective flow and inter-dendritic feeding, making the simulation more feasible with minimal computational power. More recent simulations of aluminum alloy solidification have focused more on micro-porosity, but still admit to the difficulty in predicting macro-shrinkage. [5-9]

Prediction of porosity in aluminum castings requires accurate prediction of temperatures at all locations of the casting. This is especially critical in LFC because of the unpredictable and sometimes unnatural thermal gradients that may develop after filling is complete. Moreover, the slower filling rates in LFC relative to open cavity casting result in more thermal convection, which can complicate the thermal field.

Using a finite difference method, the temperature field in a casting is governed by the internal energy:

$$V_F \frac{\partial}{\partial t}(\rho I) + \frac{\partial}{\partial x}(\rho I u A_x) + \frac{\partial}{\partial y}(\rho I v A_y) + \frac{\partial}{\partial z}(\rho I w A_z) = -p\left\{\frac{\partial u A_x}{\partial x} + \frac{\partial v A_y}{\partial y} + \frac{\partial w A_z}{\partial z}\right\} + RI_{DIF} + T_{DIF} + RI_{SOR} \quad \text{Equation 1}$$

where V_F is the volume fraction in the computational cell available for flow, A_X, A_Y, and A_Z are the fractional areas available for flow, and u, w, and w are the fluid velocities in the x, y, and z directions. The terms on the right side of the equation are related to extra heat sources and sinks. Turbulent diffusion of internal energy is as follows:

$$RI_{DIF} = \frac{\partial}{\partial x}\left(\frac{A_x c_i \mu}{\rho}\frac{\partial \rho I}{\partial x}\right) + \frac{\partial}{\partial y}\left(\frac{A_y c_i \mu}{\rho}\frac{\partial \rho I}{\partial y}\right) + \frac{\partial}{\partial z}\left(\frac{A_z c_i \mu}{\rho}\frac{\partial \rho I}{\partial z}\right) \quad \text{Equation 2}$$

where c_i is a reciprocal turbulent Prandtl Number. Heat conduction is as follows:

$$T_{DIF} = \frac{\partial}{\partial x}\left(k A_x \frac{\partial T}{\partial x}\right) + \frac{\partial}{\partial y}\left(k A_y \frac{\partial T}{\partial y}\right) + \frac{\partial}{\partial z}\left(k A_z \frac{\partial T}{\partial z}\right) \quad \text{Equation 3}$$

where T is the temperature and k is the thermal conductivity of the liquid. The internal energy shown in Equations 1 and 2 is as follows:

$$I = c_{v,l} T + (1 - f_s) c_{LHT,l} \quad \text{Equation 4}$$

where $c_{v,l}$ is the constant-volume specific heat of the liquid, f_s is the solid fraction, and $c_{LHT,l}$ is the heat of transformation. Equation 4 can be expanded further for liquids that have multiple phase transformations by lumping the phase fractions and transformation energies into the last term. [10]

Mold walls, internal cores, wall boundaries, and other such obstacles can also affect the fluid internal energy as sources or sinks. Obstacle temperatures are governed by the general heat flow equation:

$$(1 - V_F)\rho_w C_w \frac{\partial T_w}{\partial t} - \frac{\partial}{\partial x}\left[k_w (1 - A_x)\frac{\partial T}{\partial x}\right] - \frac{\partial}{\partial y}\left[k_w (1 - A_y)\frac{\partial T}{\partial y}\right] - \frac{\partial}{\partial z}\left[k_w (1 - A_z)\frac{\partial T}{\partial z}\right] = TSOR \quad \text{Equation 5}$$

where ρ_w, C_w, k_w, and T_w are solid material values for density, specific heat capacity, thermal conductivity, and temperature, respectively, and TSOR is an energy source term due to liquid-solid heat transfer and external heat sources and is equivalent to TDIF in Equation 3. [10] TSOR includes all heat energy input from phase transformations and radiative heat transfer from the liquid.

Flow-3D, produced by FlowScience, Inc., uses the equations above, as do other commercial casting simulation codes, to estimate how the temperature field will change as time progresses after completion of the LFC filling process. Isolated volumes of liquid are allowed to solidify and cavities are inserted in these hot spots in order to display predicted macro-porosity. While this physical model is accurate for rapid-fill castings and thick sections, LFC and rangy open-cavity castings do not match well with simulations. Assuming that the physical models are correct and complete, the cause of the porosity prediction inaccuracy in LFC must be due to inadequate or incorrect thermo-physical data input into the models.

EXPERIMENTAL PROCEDURES

Previous research in attempting to predict macro-porosity in aluminum-silicon LFC parts was very unsuccessful, mainly due to the inability to match cooling curve data from instrumented castings. Figure 1 shows a cooling curve from an instrumented LFC engine head casting and the corresponding simulated cooling curve from the same location. As is shown in the plot, the simulation far over-predicts the cooling in the liquid and actually predicts that there was no porosity in the casting, although the scrap rate for the part exceeded 80% because of macro-porosity. The simulation of this casting used both published thermo-physical data for A319 and data generated from a previous AFS-funded project to provide more complete thermo-physical data for casting simulations.

A closer examination of the cooling curves revealed a very basic truth about the simulated results – there was no evidence of any phase transformations in the simulated cooling curves. Figure 2 shows the enthalpy curve used as input for the simulation of the engine head. The discontinuities in the curve are not as large as they should be, considering the fact that silicon has a heat of fusion that is nearly four times that of aluminum.

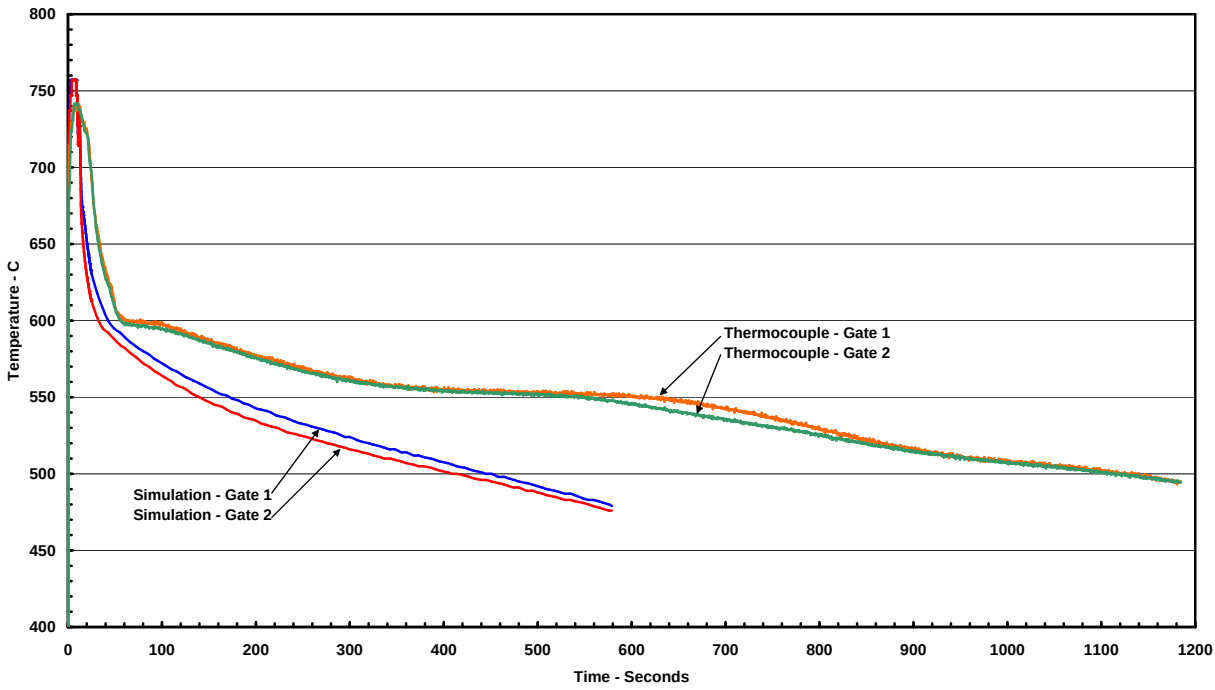

Figure 1. Simulated and experimental cooling curves from an instrumented LFC engine head casting made from A319 aluminum-silicon alloy. The simulation was run using published thermo-physical data for A319.

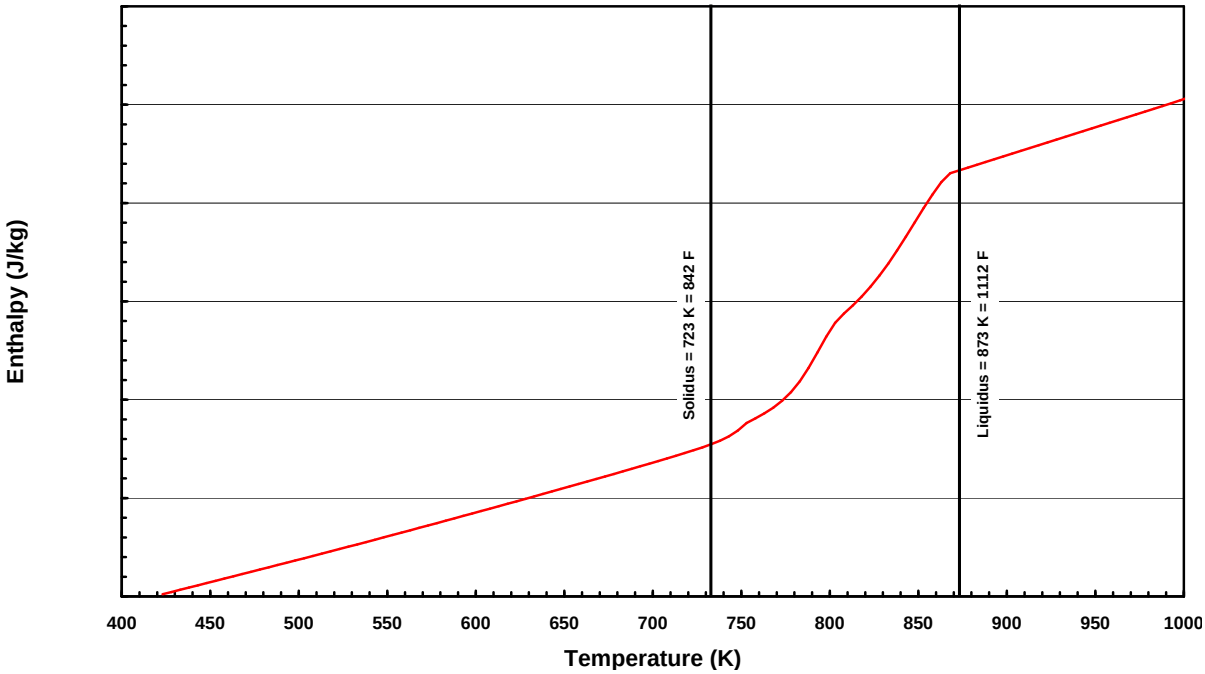

Figure 2. Enthalpy curve for A319 used to simulate the LFC head casting.

The University of Alabama at Birmingham Casting Engineering Laboratory (CEL) used a published method called the silicon equivalence method to modify the enthalpy curve. This method, along with other experiments done by the CEL, allowed the enthalpy data to be properly adjusted to account for the large enthalpy contribution from the Si-rich phases that precipitate during solidification.

Figure 3 shows the new enthalpy data produced using the Si-equivalence method. Immediately obvious is the large discontinuity that corresponds to the precipitation of the Si-rich eutectic phase. Simulations of a chemistry quick-cup match well with the experimental curve when the new enthalpy data is used, as is shown in Figure 4.

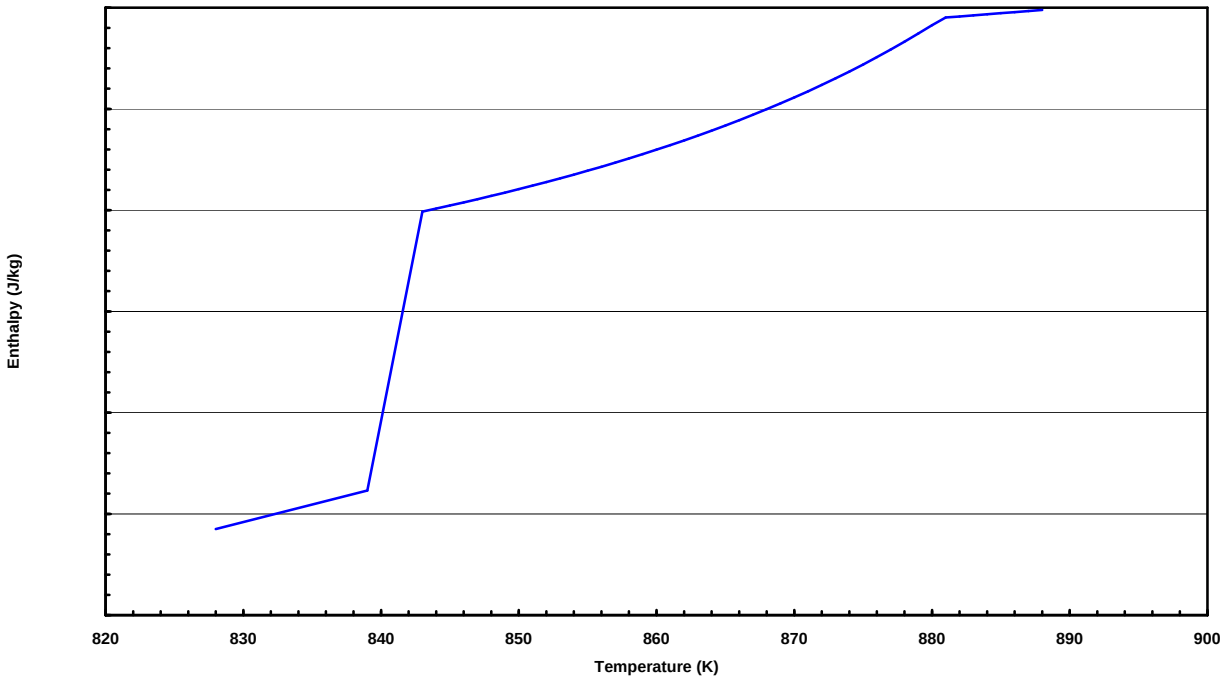

Figure 3. Plot of the new enthalpy data produced using the silicon equivalence method.

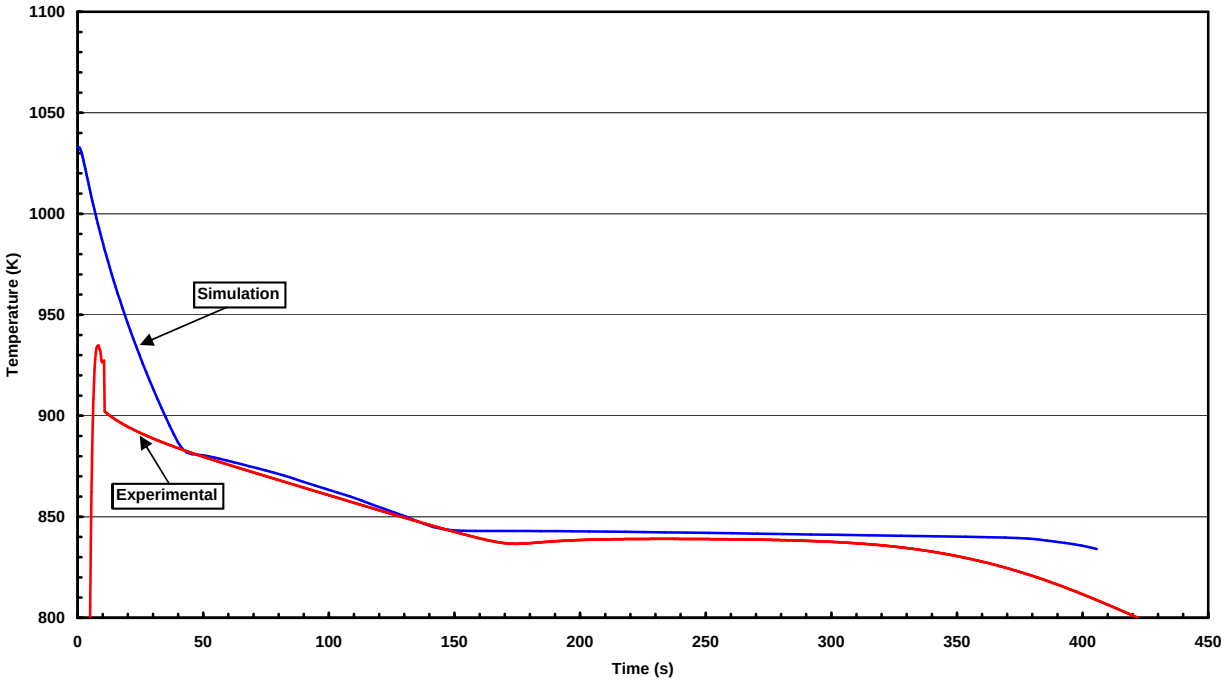

Figure 4. Plot of experimental and simulated cooling curves from a chemistry quick-cup using the new enthalpy data.

RESULTS AND DISCUSSION

Figure 5 shows images of porosity in an aluminum-silicon LFC V6 engine block and the predicted porosity location from computer simulations. The porosity shown in Figure 5a, which is colored magenta for clarity, is in the exact location as the predicted location shown in Figure 5b. In fact, the simulation correctly predicted the location of each of the macro-pores in this casting, which were nested between the cylinder bores in this casting. Previous simulations of this engine block using published enthalpy data predicted no macro-porosity in the regions shown in Figure 5 or in any other region of the casting.

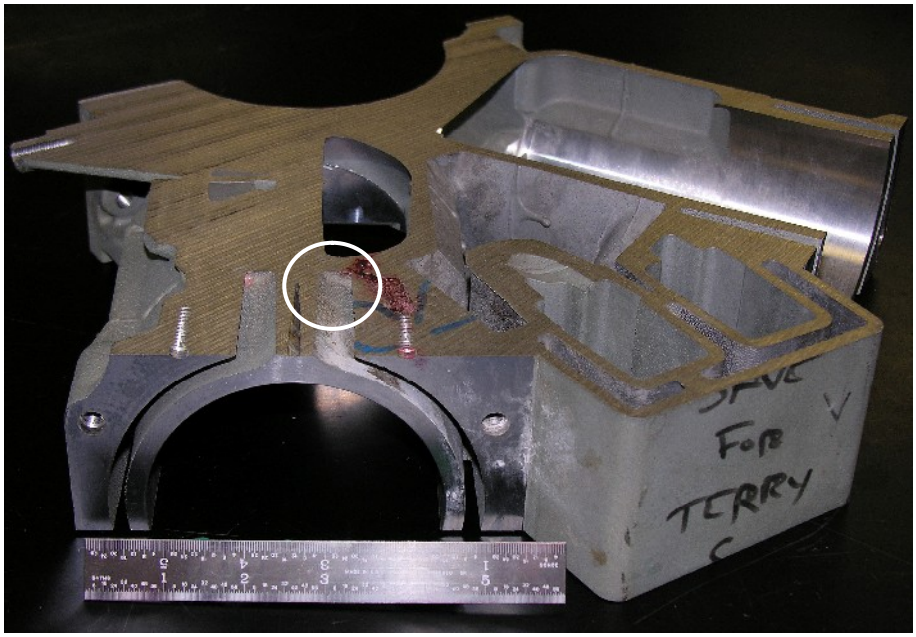

(a)

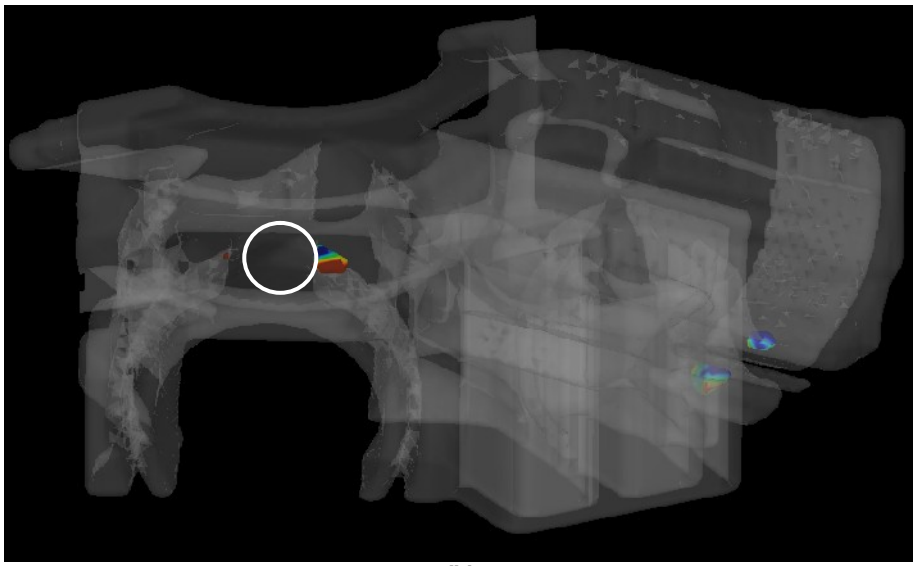

(b)

Figure 5. Image of a casting slice from an LFC engine block (a) and a simulation image from the same area (b). The colored areas in the simulation image represent the predicted macro-porosity.

Figure 6 shows slices from an in-line 6 cylinder engine block produced by LFC and poured in C356 aluminum alloy and the predicted porosity location from simulations. Simulation results shown in Figure 6b showed that there were large regions of porosity between the exhaust manifold and cylinder bores. After slicing the casting in these regions, macro-porosity was discovered where simulations indicated it would be located.

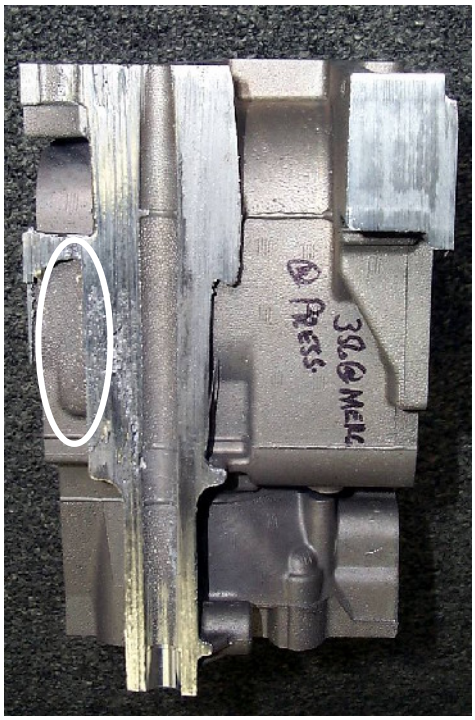

(a)

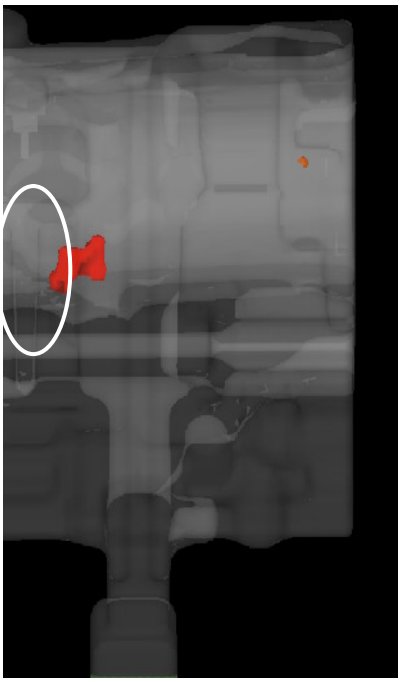

(b)

Figure 6. Casting slices showing porosity in experimental casting (a) and in a computer simulation of the same casting (b).

CONCLUSIONS

A method was developed to increase the accuracy of simulating macro-porosity in aluminum-silicon alloy castings produced by lost foam casting. Simulations of castings with high porosity scrap rates were inaccurate when published thermo-physical data was used. A modified version of the Si-equivalence method allowed much closer matching between experimental and simulated cooling curves.

The simulations showed much better accuracy in predicting macro-porosity in two different LFC production castings. Future simulation work will focus on more accurate prediction of porosity in ductile iron LFC castings as well as hypereutectic Al-Si castings.

This simulation work is intended to assist LFC aluminum and iron foundries in minimizing scrap rates by accurately simulating macro-porosity before tooling begins.

ACKNOWLEDGEMENTS

Support for this study came from the AMC PRO-ACT program sponsored by the Defense Supply Center Philadelphia, Philadelphia, PA and AFS Division 11.

REFERENCES

1. Imafuku, I. and Chijiwa, K., AFS Trans., v 91, 1983.
2. Kubo, K. and Pehlke, R.D., Metall. Trans. B, v 16B, No. 2, 1985.
3. Katzarov, I., and Popov, J., Int. J. Heat Mass Transfer, v 39, No. 14, 1996.
4. Bounds, S., Moran, G., Pericleous, K., Cross, M., and Croft, T.N., Metall. Trans. B, v 31, No. 3, 2000.
5. Huang, J., Conley, J., and Callau, P., SAE Spec. Publ., v 1336, 1998.
6. Sabau, A.S. and Viswanathan, S., Light Met., TMS Annual Meeting, 2000.
7. Carlson, K., Lin, Z., Beckermann, C., Mazurkevich, G., and Schneider, M., Model. Cast. Weld. Adv. Solidific. Proces., v 2, 2006.
8. Stefanescu, D.M., JOM, v 56, No. 11, 2004.
9. Campbell, J., Castings, Butterworth-Heinemann, 1997.
10. Flow-3D User's Manual – Theory, FlowScience, Inc.